$^3\Sigma^- - X\ ^3\Sigma^-$ Electronic Transition of Linear C_6H^+ and C_8H^+ in Neon Matrixes†

Ivan Shnitko,‡ Jan Fulara,‡,§ Anton Batalov,‡ C. Gillery,|| H. Masso,||,⊥ P. Rosmus,|| and John P. Maier*,‡

Department of Chemistry, University of Basel, Klingelbergstrasse 80, CH-4056 Basel, Switzerland, and Theoretical Chemistry, University of Marne la Vallée, France

Received: August 4, 2005; In Final Form: August 26, 2005

The electronic absorption spectra of linear C_6H^+ and C_8H^+ were recorded in 6 K neon matrixes following mass selective deposition. The (1) $^3\Sigma^- - X\ ^3\Sigma^-$ electronic transition is identified with the origin band at 515.8 and 628.4 nm for l-C_6H^+ and l-C_8H^+, respectively. One strong (near 267 nm) and several weaker electronic transitions of l-C_8H^+ have also been observed in the UV. The results of ab initio calculations carried out for linear and cyclic C_6H^+ are consistent with the assignment.

Introduction

C_nH are the second longest carbon chains after cyanopolyynes detected in the interstellar medium (ISM).[1] These radicals were observed both in dark molecular clouds[2] and in envelopes of carbon rich stars.[3] Despite the higher reactivity of the open shell C_nH species, their abundance in these environments is only slightly lower than the same sized closed shell $H(CC)_nCN$ molecules.

The C_nH radicals have been extensively studied in the microwave and visible spectral ranges. Chains up to $n \leq 14$ were generated in an electrical discharge through a mixture of diacetylene with neon and identified using rotational spectroscopy.[4,5] Electronic absorption spectra of $C_{2n}H$, $3 \leq n \leq 8$, have been measured in neon matrixes[6] and in the gas phase up to $n = 6$ using cavity ring down methods.[7−9] The medium size chains $n = 2-4$ have also been studied using theoretical methods.[10−13] These reveal two close lying $^2\Sigma$ and $^2\Pi$ electronic states, the latter being the lowest for $n \geq 3$.

In contrast to the C_nH neutral radicals, little is known about their molecular ions. The reaction of medium size C_nH^+ ($n = 2-6$) with CO was studied using mass spectrometry.[14] However, only the smallest member of this group CH^+ has been characterized spectroscopically,[15] which was also detected long ago in diffuse interstellar clouds by its A $^1\Pi - X\ ^1\Sigma^+$ electronic transition.[16] In view of the significant abundance of the neutral counterparts in the ISM, one would also expect that C_nH^+ should be present. Therefore their spectroscopic characterization is a prerequisite. This paper is the first experimental report on the electronic spectra of linear C_6H^+ and C_8H^+ that have been observed in 6 K neon matrixes. No theoretical study on the electronically excited states for these two cations has been reported.

Experimental Section

The measurements were carried out using the approach of mass selection combined with matrix absorption spectroscopy.[17] The ions were produced in a hot cathode discharge source and accelerated to about 50 eV. The C_nH^+ ions were mass selected with a quadrupole and deposited with an excess of neon on a rhodium-coated sapphire plate at 6 K. The resolution of the mass filter was ±1 amu to obtain a sufficient current. The matrix was grown for 2 h, after which the absorption spectrum was measured in the 220−1100 nm region using a waveguide technique[18] with a xenon arc or halogen lamp light source, a monochromator, and a photomultiplier or silicon diode detector. To neutralize charged molecules, the surface of the matrix was irradiated with a medium-pressure mercury lamp after deposition.

Theory

The influence of atomic orbital basis sets, active orbitals in CASSCF approach, and reference wave functions for internally contracted MRCI calculations on the precision for the electronic excitation energy and transition moment was previously investigated in an extensive theoretical study on C_6^+.[19] Because most of the excited states have strongly multiconfigurational character, accurate calculations of these properties in cumulenic carbon chains remain a difficult problem.

On the basis of the experience with C_6^+, the following computational scheme was adapted for C_6H^+. The geometry optimizations of several states were performed with the aug-cc-pVTZ basis set of Dunning[20,21] and the CASSCF[22] method. The 5-8σ, 1-4π orbitals were active for the linear structure and 5-11a_1, 2-4b_1, 4-7b_2, 1-2a_2 for the cyclic one. Excitations from lower orbitals were not considered. The following equilibrium geometries were calculated for the linear structure of C_6H^+ (all distances in Å for R_i, $i = 1-6$, Figure 1): X $^3\Sigma^-$ 1.299, 1.280, 1.263, 1.297, 1.212, and 1.082; $2^3\Sigma^-$ 1.309, 1.290, 1.267, 1.259, 1.283, and 1.083; $1^3\Pi$ 1.234, 1.314, 1.223, 1.339, 1.192, and 1.079. In the case of the C_{2v} cyclic structure (R_i, $i = 1-4$, and angles in degrees for α_i, $i = 1-3$, cf. Figure 1): X^1A_1 1.067, 1.371, 1.287, 1.313, 131.8, 142.7, and 94.4; 1^1B_1 1.071, 1.446, 1.292, 1.307, 123.2, 122.4, and 115.0; 1^1B_2 1.068, 1.358, 1.301, 1.358, 135.5, 142.2, and 118.8. The ground-state geometries of the linear and cyclic ground state of C_6H^+ from an earlier study[22] are in overall agreement with the present results, though some bond distances differ by up to 0.048 Å.

The vertical and adiabatic excitation energies were all calculated in the C_{2v} point group. Four states in each irreducible

† Part of the special issue "Jürgen Troe Festschrift".

* Corresponding author. E-mail: j.p.maier@unibas.ch. Phone: +41 61 267 38 26. Fax: +41 61 267 38 55.

‡ University of Basel.

§ Permanent address: Institute of Physics, Polish Academy of Sciences, Al. Lotników 32-46, Pl-02668 Warsaw, Poland.

|| University of Marne la Vallée, France.

⊥ Permanent address: DAMIR-IEM-CSIC, Madrid, Spain.

10.1021/jp054331f CCC: $33.50
Published on Web 10/05/2005

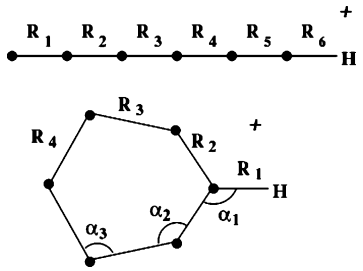

Figure 1. Definition of the coordinates for linear and cyclic C_6H^+. The calculated distances and angles for the ground and excited states are given in the text.

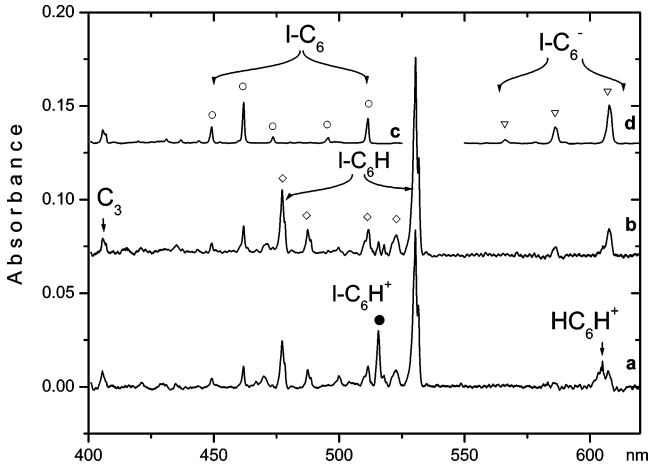

Figure 2. Electronic transition of l-C_6H^+ (●) observed in a 6 K neon matrix after deposition of C_6H^+ produced from C_6Cl_5H (trace **a**) and subsequent UV irradiation (trace **b**). The electronic absorption bands of l-C_6H (◇) are also present as a result of the neutralization and capture of electrons by C_6H^+. To facilitate the identification of the bands in trace **b**, the previously obtained electronic spectra of l-C_6 and l-C_6^- are shown in traces **c** and **d**.

representation were averaged together in the CASSCF calculations comprising about 4.3×10^6 CSF's (triplets) or 2.3×10^6 CSF's (singlets) with an active space 5-9σ, 1-5π orbitals for the linear structure. An active space consisting of 5-11a_1, 1-4b_1, 4-7b_2 and 1-2a_2 orbitals was used in the case of the cyclic structure. In the calculations of the adiabatic excitation energies for l-C_6H^+, the lowest σ orbital from the space defined above was closed; for c-C_6H^+ the active space remained unchanged. All calculations were performed with the MOLPRO code.[23] More comprehensive information can be found in ref 24.

Results and Discussion

Electronic Spectrum of C_6H^+. The electronic absorption spectrum recorded after deposition of mass selected C_6H^+ in a 6 K neon matrix is shown in trace **a** of Figure 2. The cations were generated in the source from pentachlorobenzene, C_6Cl_5H, as the precursor. A photobleaching procedure was used to distinguish the absorption bands of cations from those of neutral species. In this the matrix was irradiated with UV photons ($\lambda \geq 305$ nm) and the spectrum was recorded anew, leading to trace **b**. Most of the bands seen in trace **a** increase in intensity after irradiation except for the peaks at 515.8 nm and that of HC_6H^+ at 604 nm which both diminish. The bands that increase originate from known species, namely, linear C_6, C_6H, and C_6^-.[25] To facilitate the identification of these bands, the previously obtained electronic spectra of l-C_6 and l-C_6^- are shown in traces **c** and **d**.

The origin band of the A $^2\Pi_g - X\ ^2\Pi_u$ band system of the triacetylene cation, HC_6H^+, is seen weakly in trace **a** as a

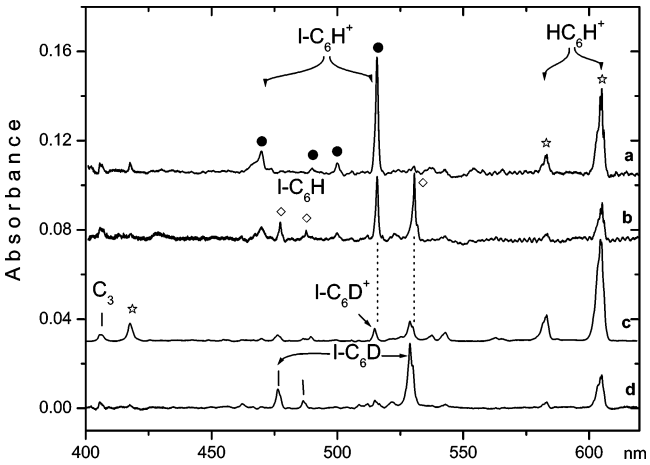

Figure 3. Electronic transition of l-C_6H^+ (●) observed in the visible region after deposition of mass-selected C_6H^+ in a matrix containing 0.25% N_2O (trace **a**). Trace **b** shows the spectrum recorded after UV irradiation; the bands that grow in intensity originate from l-C_6H (◇). Apart from l-C_6H^+, the electronic absorption bands of $C_6H_2^+$ (☆) are also present in trace **a** due to the low mass resolution (±1 amu) used. C_6D^+ was produced from dideuteriodiacetylene. The spectrum recorded after deposition is shown in trace **c** and after subsequent UV irradiation in trace **d**.

result of the limited mass resolution (±1 amu) and the contamination of the C_6Cl_5H sample with chlorobenzenes containing more than one hydrogen atom. l-C_6 and C_3 (at 405 nm) are present in the matrix as a result of collisionally induced fragmentation of the C_6H^+ cations during deposition. Another reason for the presence of l-C_6 can be the charge neutralization of C_6^+, which is co-deposited with C_6H^+ due to the low mass resolution. However, the known absorption[26] of C_6^+ was not detected.

After irradiation of the matrix, the origin band of HC_6H^+ and the new distinct band at 515.8 nm diminish while the l-C_6H bands grow in intensity (trace **b** of Figure 2). The absorptions of l-C_6 increase only slightly while those of l-C_6^- appear. The electrons that are detached from weakly bound anions by UV photons migrate in the matrix and, on meeting cations, neutralize them. This is the reason the l-C_6H bands become stronger. The neutralization of l-C_6H^+ with electrons is an exoenergetic process and some excited l-C_6H molecules undergo a fragmentation, being responsible for the slight growth in intensity of the l-C_6 bands upon irradiation. l-C_6 does not appear to be produced by neutralization of C_6^+ because its absorption was not detected. Some of the liberated electrons are captured by molecules with a high electron affinity, e.g., l-C_6. This process leads to the appearance of the C_6^- bands (trace **b**).

A small amount of N_2O (0.25%) was added to neon to improve the trapping efficiency of the C_6H^+ cations during deposition. The resulting spectrum is shown in trace **a** of Figure 3. A large difference in the intensity of the bands is evident on comparing traces **a** of Figures 2 and 3, though the C_6H^+ deposition ion current was comparable. The absorptions of neutral species are nearly absent in trace **a** of Figure 3 whereas the 515.8 nm peak and the origin of HC_6H^+ become much stronger. These differences point to a cationic carrier of the 515.8 nm band. The strengthening of the cationic absorptions and weakening of the neutrals' ones was previously observed in the study of the electronic absorption spectra of C_n^+ ($n = 6-9$) trapped in neon matrixes containing N_2O.[26,27] The latter is a scavenger for electrons that are released from metal surfaces by collisions with cations being deposited. As a result, the density of free electrons in the matrix is reduced and the

neutralization efficiency of deposited cations suppressed. Therefore neutral species (l-C_6H) are nearly absent in the matrix containing N_2O.

The matrix was then irradiated with $\lambda \geq 305$ nm photons, leading to trace **b** of Figure 3. The bands of HC_6H^+ and the system with the onset at 515.8 nm diminish, while the absorption of neutral l-C_6H appears. One can therefore conclude that the 515.8 nm band system originates from C_6H^+. The oscillator strength of this electronic transition of C_6H^+ is estimated to be comparable to that of the $2\ ^2\Pi - X\ ^2\Pi$ electronic transition of l-C_6H, calculated to be $\sim$0.02.[12,13]

Further experiments have been carried out in which linear and cyclic C_6^+ were generated from perchlorobenzene, mass selected, and trapped in a neon matrix containing 1% H_2. The 515.8 nm absorption band was detectable. It is known from gas-phase[28,29] and matrix experiments[26] that l-C_6^+ is more reactive than its cyclic isomer. Therefore one can expect that linear C_6H^+ was formed in the matrix by the reaction of l-C_6^+ with H_2. The recent studies on C_6^+ show that the structure of the cations depends on the precursor used for their generation. The linear and cyclic isomers of C_6^+ were formed from perchlorobenzene, whereas solely the cyclic one was formed from perbromobenzene.[26]

In the next experiment cations of mass 74 were generated from dideuteriodiacetylene precursor. The spectrum recorded after deposition is shown in trace **c** and after subsequent UV irradiation in trace **d** of Figure 3. The $A\ ^2\Pi_g - X\ ^2\Pi_u$ system of HC_6H^+ and the band of C_6D^+ around 515 nm are observed, both ions having the same mass. Trace **c** is scaled by a factor of 0.2 to obtain the same intensity of the origin band of HC_6H^+ (☆ in traces **a**, **c**) for a better visual comparison.

After $\lambda \geq 305$ nm irradiation the bands of the cations diminish and the l-C_6D system grows in intensity (trace **d** of Figure 3). Trace **d** was normalized to the intensity of the origin band of l-C_6D for comparison with plot **b**. The origin bands of l-C_6D and C_6D^+ are shifted to the blue by 1.6 and 1 nm with respect to the l-C_6H and C_6H^+ species, respectively. The l-C_6D/l-C_6H gas-phase shift is 1.424 nm.[8]

These results indicate that only one isomer of $C_6H(D)^+$ with the band origin around 515 nm was observed in a neon matrix, irrespective of the precursor (C_6Cl_5H or DC_4D) or of the production method (electron impact ionization or the reaction of l-C_6^+ with H_2). This suggests that it is the linear $C_6H(D)^+$. The electronic absorption spectrum of this cation is simple and comprises the 515 nm origin and three weaker vibronic bands. Their assignment in Table 1 is made by comparison to the calculated vibrational frequencies of l-C_6H.[13]

l-C_6H^+ is isoelectronic with l-C_6. The ground-state electronic configuration of l-C_6 is $...1\pi_u^4\ 6\sigma_u^2\ 7\sigma_g^2\ 1\pi_g^4\ 2\pi_u^2$, which leads to a $X\ ^3\Sigma_g^-$ electronic ground state.[30] l-C_6H^+ has a lower symmetry with configuration $...1\pi^4\ 12\sigma^2\ 2\pi^4\ 13\sigma^2\ 3\pi^2$. The hydrogen atom in this cation will mostly affect the energy of the σ orbitals. The main difference in the electronic spectra of l-C_6 and l-C_6H^+ will be caused by a promotion of an electron from the $12\sigma^2$ and $13\sigma^2$ orbital. The strongest (1) $^3\Sigma_u^- \leftarrow X\ ^3\Sigma_g^-$ electronic transition of l-C_6 with the onset at 511 nm[25] results from the $1\pi_g \rightarrow 2\pi_u$ excitation. One can also expect that the corresponding $2\pi \rightarrow 3\pi$ promotion will be responsible for the electronic transition of l-C_6H^+ in the similar spectral range. Indeed, the origin band of the l-C_6H^+ (515.8 nm) absorption system lies close to the (1) $^3\Sigma_u^- \leftarrow X\ ^3\Sigma_g^-$ electronic transition of l-C_6 (origin at 511 nm).

Theoretical Prediction for C_6H^+. Previously it was shown that for the linear structures there is a low lying $^3\Pi$ state close to $X\ ^3\Sigma^-$ in C_6 or $^2\Sigma^+$ ($13\sigma \rightarrow 3\pi$) in C_6H.[13] This state has been detected experimentally for C_6H 0.18 eV above the $X\ ^2\Pi$ state.[31] In the present CASSCF calculations on C_6H^+ the two states lie even closer (Figure 4); at equilibrium geometries the $^3\Pi$ state is predicted to lie lower than $^3\Sigma^-$ by 0.04 eV. It is calculated that due to strong changes of the π orbital system the transition $2^3\Pi \leftarrow 1^3\Pi$ with $T_v = 2.36$ eV has a large transition moment of 3.2 D. To obtain a more reliable estimate on the relative positions of the ground state, RCCSD(T)/cc-pVQZ calculations were performed at the optimized geometries of the lowest $^3\Pi$, $^3\Sigma^-$, and $^1A_1$ states, in which all 24 valence electrons were correlated. The cyclic X^1A_1 state is found to be 0.51 eV more stable than the linear $X\ ^3\Sigma$, and 0.84 eV more stable than the $^3\Pi$ state. The electronic ground state has $^3\Sigma^-$ symmetry in the linear geometry. At higher energies the multidimensional potential energy surfaces of both triplets can exhibit avoided crossings and vibronic couplings.

The pattern of CASSCF vertical excitation energies for the triplets and singlets of the linear and cyclic structure of C_6H^+ is shown in Figure 4. These are plotted relative to the RCCSD-(T) energies for equilibrium geometries of the $X\ ^3\Sigma^-$ or X^1A_1 states. The strongest transition in the linear triplets is $^3\Sigma^- \leftarrow X^3\Sigma^-$ calculated at 2.92 eV (adiabatic 2.77 eV) with a moment of 1.48 D. This energy difference is higher than the

TABLE 1: Observed Bands (±0.2 nm) in the Electronic Absorption Spectra of l-C_6H^+, l-C_6D^+ and l-C_8H^+ in 6 K Neon Matrixes and the Suggested Assignments[a]

species	λ/nm	ν/cm^{-1}	Δ/cm^{-1}	assignment	
l-C_6H^+	515.8	19387	0	0_0^0	(1) $^3\Sigma^- - X\ ^3\Sigma^-$
	500.0	20000	613	ν_6	
	489.8	20416	1029	ν_5	
	469.7	21290	1903	ν_4	
l-C_6D^+	514.8	19425	0	0_0^0	(1) $^3\Sigma^- - X\ ^3\Sigma^-$
	499.4	20024	599	ν_6	
	469.7	21290	1865	ν_4	
l-C_8H^+	628.4	15913	0	0_0^0	(1) $^3\Sigma^- - X\ ^3\Sigma^-$
	610.2	16388	475	ν_8	
	564.5	17715	1802	ν_5	
	549.1	18212	2299	$\nu_5 + \nu_8$	
	379.3	26364	0	0_0^0	$B - X\ ^3\Sigma^-$
	372.2	26867	503	ν_8	
	357.9	27941	1577	ν_6	
	355.1	28161	1797	ν_5	
	351.9	28417	2053	ν_4	
	349.2	28637	2273	$\nu_5 + \nu_8$	
	346.5	28860	2496	$\nu_4 + \nu_8$	
	327.8	30506	0	0_0^0	$C - X\ ^3\Sigma^-$
	323.0	30960	454	ν_8	
	318.0	31447	941	ν_7	
	314.1	31837	0	0_0^0	$D^* - X\ ^3\Sigma^-$
	309.2	32342	505	ν_8	
	304.7	32819	982	ν_7	
	299.9	33344	1507	ν_6	
	296.7	33704	1867	ν_5	
	292.6	34176	2339	$\nu_5 + \nu_8$	
	289.1	34590	2753	$\nu_5 + \nu_7$	
	285.3	35051	3214		
	281.7	35499	3662	$2\nu_5$	
	267.1	37439	0		$E\ ^3\Sigma^- - X\ ^3\Sigma^-$
	263.6	37936	497	ν_8	
	253.7	39417	1978	ν_4	
	250.4	39936	2497	$\nu_4 + \nu_8$	
	242.7	41203	3764	$2\nu_4$	

[a] The letters in the last column refer to the excited electronic states indicated in Figures 5 and 6. l-C_6H: (σ) $\nu_1 = 3457$, $\nu_2 = 2137$, $\nu_3 = 2105$, $\nu_4 = 1895$, $\nu_5 = 1224$, $\nu_6 = 650$ cm^{-1}; (π) $\nu_8 = 567$, $\nu_9 = 570$, $\nu_{10} = 397$, $\nu_{11} = 210$, $\nu_{12} = 93$ cm^{-1}.[13] l-C_8: (σ) 2168 (u), 2144 (g), 2032 (g), 1770 (u), 1404 (g), 979 (u), 516 (g) cm^{-1}; (π) 706 (g), 584 (u), 413 (g), 264 (u), 160 (g), 65 (u) cm^{-1} [26]. * − tentative.

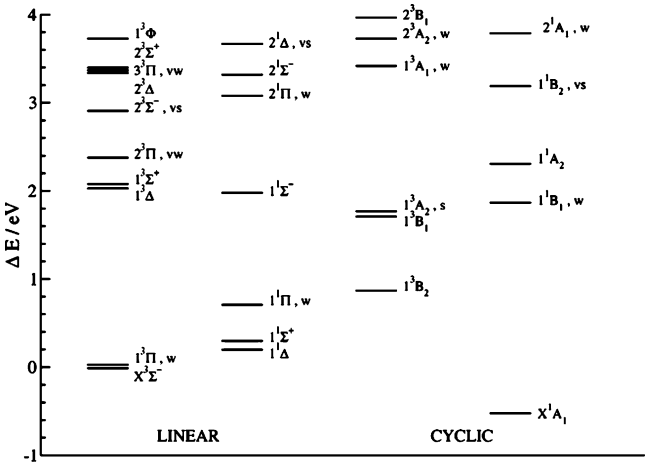

Figure 4. CASSCF vertical electronic excitation energies for linear and cyclic C_6H^+ relative to the RCCSD(T) energy of the $X\ ^3\Sigma^-$ (linear) state at its equilibrium geometry. The strengths of allowed transition are indicated by vw = very weak, w = weak, s = strong, and vs = very strong.

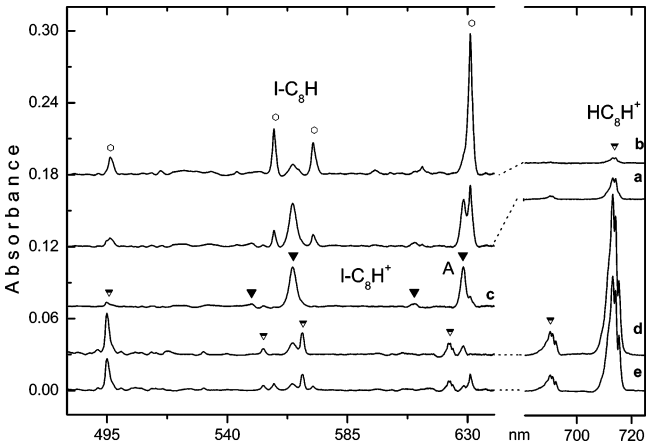

Figure 5. Electronic transition of $l\text{-}C_8H^+$ (▼) observed after deposition of mass-selected C_8H^+ in a 6 K neon matrix from diacetylene (trace **a**). Trace **b** shows the spectrum recorded after UV irradiation; the bands that grow in intensity originate from l-C_8H (○). Trace **c** shows the spectrum obtained after subtracting bands of l-C_8H. Trace **d** shows the absorptions after deposition of C_8H^+ in a neon matrix containing N_2O (0.25%), and trace **e** was obtained after irradiation. The top-filled down-pointing triangle indicates the bands of $l\text{-}C_8H_2^+$.

experimental value of 2.4 eV due to the missing electron correlation contribution in the present ansatz. The $^3\Pi \leftarrow X\ ^3\Sigma^-$ transition at 2.39 eV vertical excitation (adiabatic 2.24 eV) has only a small moment of 0.02 D and thus cannot be responsible for the rather intense feature detected experimentally. Similarly, the $1^1B_1 \leftarrow X^1A_1$ transition at 2.39 eV (adiabatic 1.82 eV) has a smaller moment of 0.43 D. Hence the pattern of allowed transitions advocates the assignment of the band at 515.8 nm to the linear isomer. The schemes of the electronic states of linear C_6 and its protonated form C_6H^+ are analogous, although the ordering differs for higher energy states. The largest change in the ground states is the strong distortion of the C_6H^+ cyclic form relative to the neutral C_6 ring.

Electronic Spectrum of C_8H^+. C_8H^+ was produced in the ion source from a mixture of diacetylene with helium (1:3). The known absorptions of linear C_8H with the onset at 631 nm[6] and a weak band system of tetraacetylene cation, HC_8H^+, with the origin at 714 nm[17] are present in trace **a** (Figure 5). The l-C_8H bands grow in intensity while the peaks of the HC_8H^+ cation diminish substantially upon UV irradiation (trace **b**).

Apart from l-C_8H and HC_8H^+, a new band system with the origin at 628.4 nm is discernible in trace **a**. This absorption diminishes upon UV irradiation similarly as the ones of HC_8H^+ (trace **b**). The new band system partially overlaps with the absorption of l-C_8H. Trace **c** shows the spectrum obtained after subtracting the bands of l-C_8H. Two absorptions with origin at 628.4 nm and one at 564.5 nm (i.e., 1802 cm^{-1} to higher energy) dominate in this spectrum. These bands have a peculiar intensity distribution because they are equally strong but no overtone transition around 512 nm ($2 \times 1802\ cm^{-1}$) could be detected.

To check whether these bands belong to one or two isomers of C_8H^+, an additional experiment was carried out. C_8H^+ was trapped in a neon matrix containing N_2O (0.25%) as the electron scavenger and reactant of C_8H^+. Trace **d** (Figure 5) shows the absorptions after deposition and trace **e** after irradiation. No absorptions of l-C_8H are present in trace **d**, which indicates that the neutralization of C_8H^+ was completely suppressed. The bands at 628.4 and 564.5 nm are clearly seen in trace **d** and they diminish upon irradiation (trace **e**). Although these peaks are weaker than those in in trace **a**, their relative intensity remains the same as those in the experiment without scavenger. These results suggest that the 628.4 and 564.5 nm bands originate from the same isomer of C_8H^+. Apart from the bands of C_8H^+, a strong absorption of HC_8H^+ is also observed in trace **d**. The intensity of the HC_8H^+ absorption is much higher than in trace **a**, due to a lower mass resolution used in this experiment and/or consumption of C_8H^+ in the reaction with N_2O in the matrix. The linear isomer of C_8H^+ is expected to be more reactive than the cyclic one.

The origin band of C_8H^+ (at 628.4 nm) lies close to that of the (1) $^3\Sigma_u^- - X\ ^3\Sigma_g^-$ electronic transition of the isoelectronic l-C_8, at 639.8 nm.[6] Because C_8H^+ was produced from the linear precursor (HC_4H), one can expect that the linear geometry will be preserved in the C_8H^+ cation. Thus it is concluded that the new band system with the onset at 628.4 nm is due to the $^3\Sigma^- - X\ ^3\Sigma^-$ electronic transition of $l\text{-}C_8H^+$. The oscillator strength of this transition is about 2 times smaller than that for l-C_8H with the onset at 631 nm.[6]

The wavelengths of the observed absorption bands in the electronic spectrum of $l\text{-}C_8H^+$ are given in Table 1. The vibrational assignment is based on the theoretical calculations for l-C_8.[32] The calculated ground-state frequencies of l-C_8 and those observed in the excited electronic state of $l\text{-}C_8H^+$ are in reasonable accord. The numbering of the modes differs: $l\text{-}C_8H^+$ has three more vibrations than l-C_8 (one of σ symmetry (ν_1) around 3000 cm^{-1} and two doubly degenerate π modes). The band at 564.5 nm corresponds to the ν_5 vibrational excitation in the $^3\Sigma^-$ electronic state of $l\text{-}C_8H^+$. Two weaker bands (trace **c**) correspond to the ν_8 vibration and the combination with the ν_5 mode.

Traces **a** of Figures 5 and 6 were recorded in the same experiment. Trace **b** represents another measurement in which the ion current was lower, and the bands are therefore weaker. They vanish after UV irradiation (trace **c**). Trace **d** was recorded after deposition of C_8H^+ with an admixture of N_2O. The bands seen in trace **d** are weak similar to those of $l\text{-}C_8H^+$ seen in the visible part (Figure 5). None of the absorption peaks in trace **d** of Figure 6 originate from HC_8H^+ because the visible bands of this cation are much stronger than in trace **a**. Thus the rich absorption system seen in trace **a** of Figure 6 is due to $l\text{-}C_8H^+$.

One can distinguish at least three electronic transitions of $l\text{-}C_8H^+$ in the UV spectral range (trace **a** of Figure 6). The clear origin bands of these are at 379.3, 327.8, and 267.1 nm. The strongest band system lies close to the (2) $^3\Sigma_u^- - X\ ^3\Sigma_g^-$

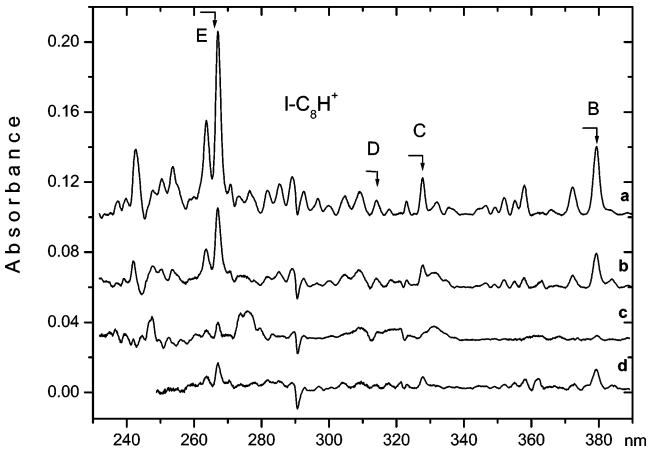

Figure 6. UV electronic transition of l-C_8H^+ observed in 6 K neon matrixes generated from diacetylene. Trace **a** was recorded in the same experiment as trace **a** of Figure 3. Trace **b** represents another experiment in which the ion current was lower. Trace **c** shows the spectrum recorded after UV irradiation. The spectrum recorded after deposition of C_8H^+ with an admixture of N_2O is shown in trace **d**.

transition of the isoelectronic l-C_8 molecule (at 277.2 nm).[30] A weaker $^3\Pi_u - X\ ^3\Sigma_g^-$ system of l-C_8 lies at 303.6 nm. l-C_8H^+ has one, or two, electronic transitions (C and D) in this spectral region.

Conclusions

The $^3\Sigma^- - X\ ^3\Sigma^-$ electronic transitions of linear C_6H^+ and C_8H^+ in the visible spectral region are close to those of the isoelectronic C_n, n= 6, 8, carbon chains with oscillator strengths similar to the ones of l-C_nH, n = 6, 8. Several electronic transitions in the UV range of l-C_8H^+ are also observed, and the strongest at 267.1 nm has a counterpart in the l-C_8 spectrum. The identification of the electronic spectra of these astrophysically important species in neon matrixes is a good starting point for gas-phase studies.

Acknowledgment. This work has been supported by the Swiss National Science Foundation (project 200020-100019) and the EU project Molecular Universe (MRTN-CT-2004-512302).

References and Notes

(1) Guélin, M.; Cernicharo, J.; Kahane, C.; Gomez-Gonzalez, J.; Walmsley, C. M. *Astron. Astrophys.* **1987**, *175*, L5.

(2) Guélin, M.; Cernicharo, J.; Travers, M. J.; McCarthy, M. C.; Gottlieb, C. A.; Thaddeus, P.; Ohishi, M.; Saito, S.; Yamamoto, S. *Astron. Astrophys.* **1997**, *317*, L1.

(3) Cernicharo, J.; Guélin, M. *Astron. Astrophys.* **1996**, *309*, L27.

(4) McCarthy, M. C.; Travers, M. J.; Kovàcs, A.; Gottlieb, C. A.; Thaddeus, P. *Astron. Astrophys.* **1996**, *309*, L31.

(5) Gottlieb, C. A.; McCarthy, M. C.; Travers, M. J.; Grabow, J.-U.; Thaddeus, P. *J. Chem. Phys.* **1998**, *109*, 5433.

(6) Freivogel, P.; Fulara, J.; Jakobi, M.; Forney, D.; Maier, J. P. *J. Chem. Phys.* **1995**, *103*, 54.

(7) Kotterer, M.; Maier, J. P. *Chem. Phys. Lett.* **1997**, *266*, 342.

(8) Linnartz, H.; Motylewski, T.; Vaizert, O.; Maier, J. P.; Apponi, A. J.; McCarthy, M. C.; Gottlieb, C. A.; Thaddeus, P. *J. Mol. Spectrosc.* **1999**, *197*, 1.

(9) Linnartz, H.; Motylewski, T.; Maier, J. P. *J. Chem. Phys.* **1998**, *109*, 3819.

(10) Pauzat, F.; Ellinger, Y. *Astron. Astrophys.* **1989**, *216*, 305.

(11) Woon, D. E. *Chem. Phys. Lett.* **1995**, *244*, 45.

(12) Sobolewski, A. L.; Adamowicz, L. *J. Chem. Phys.* **1995**, *102*, 394.

(13) Cao, Z.; Peyerimhoff, S. D. *Phys. Chem. Chem. Phys.* **2001**, *3*, 1403.

(14) Bohme, D. K.; Wlodek, S.; Williams, L.; Forte, L.; Fox, A. *J. Chem. Phys.* **1987**, *87*, 6934.

(15) Douglas, A. E.; Herzberg, G. *Astrophys. J.* **1941**, *94*, 381.

(16) Adams, W. S. *Astrophys. J.* **1949**, *109*, 354.

(17) Freivogel, P.; Fulara, J.; Lessen, D.; Forney, D.; Maier, J. P. *Chem. Phys.* **1994**, *189*, 335.

(18) Rossetti, R.; Brus, L. E. *Rev. Sci. Instrum.* **1980**, *51*, 467.

(19) Gillery, C.; Rosmus, P.; Werner, H.-J.; Stoll, H.; Maier, J. P. *Mol. Phys.* **2004**, *102*, 2227.

(20) Dunning, T. H. *J. Chem. Phys.* **1989**, *90*, 1007.

(21) Kendall, R. A.; Dunning, T. H.; Harrison, R. J. *J. Chem. Phys.* **1992**, *96*, 6796.

(22) Fehèr, M.; Maier, J. P. *Chem. Phys. Lett.* **1994**, *227*, 371.

(23) Werner, H.-J.; Knowles, P. J. *Molpro program, further information can be obtained from http:/www.molpro.net/*.

(24) Gillery, C. Ph.D. Thesis, University of Marne la Vallée, France, 2005.

(25) Forney, D.; Fulara, J.; Freivogel, P.; Jakobi, M.; Lessen, D.; Maier, J. P. *J. Chem. Phys.* **1995**, *103*, 48.

(26) Fulara, J.; Riaplov, E.; Batalov, A.; Shnitko, I.; Maier, J. P. *J. Chem. Phys.* **2004**, *120*, 7520.

(27) Fulara, J.; Shnitko, I.; Batalov, A.; Maier, J. P. *J. Chem. Phys.* **2005**, *123*, 044305.

(28) Sowa-Resat, M. B.; Smolanoff, J. N.; Goldman, I. B.; Anderson, S. L. *J. Chem. Phys.* **1994**, *100*, 8784.

(29) McElvany, S. W.; Dunlap, B. I.; O'Keefe, A. *J. Chem. Phys.* **1987**, *86*, 715.

(30) Grutter, M.; Wyss, M.; Riaplov, E.; Maier, J. P.; Peyerimhoff, S. D.; Hanrath, M. *J. Chem. Phys.* **1999**, *111*, 7397.

(31) Taylor, T. R.; Xu, C.; Neumark, D. M. *J. Chem. Phys.* **1998**, *108*, 10018.

(32) Martin, J. M. L.; El-Yazal, J.; Francois, J. P. *Chem. Phys. Lett.* **1995**, *242*, 570.